Solution-Phase ^{13}C and ^{1}H Chemical Shift Anisotropy of Sialic Acid and Its Homopolymer (Colominic Acid) from Cross-Correlated Relaxation†

Gyula Batta‡ and Jacquelyn Gervay*

Contribution from the University of Arizona, Department of Chemistry, Tucson, Arizona 85721

Received December 23, 1993®

Abstract: Sensitive pulse sequences were developed in order to determine geometry dependent ^{1}H and ^{13}C chemical shift anisotropy terms (CSA_g) of simple carbohydrates and carbohydrate polymers in solution. The methods are capable of monitoring CSA/DD cross-correlated relaxation for ca. 1 M solutions at natural abundance. Measured spectral densities were quantitatively interpreted for sialic acid and its α-(2→8) linked homopolymer, colominic acid. Although the geometric factors could not be separated from anisotropy terms, this is the first report of CSA data on a carbohydrate polymer, and its values differ substantially from those of monomeric sialic acid. The most pronounced differences were observed at C5, C6, and C7 for both ^{1}H- and ^{13}C-shift anisotropies. The differences may be attributed to conformational changes around the C6/C7 and C7/C8 bonds, and possible changes in hydrogen bonding interactions, and in OH rotamer populations. Application of these combined NMR methods provide a new parameter which may be sensitive to structural changes not detected with conventional NMR techniques.

Introduction

Sialoglycoconjugates are a class of sialic acid containing carbohydrates which are intimately involved in cellular recognition processes involving protein/carbohydrate interactions.[1] It would be extremely useful from the perspective of biomimetic design to be able to detect structural changes occurring in the carbohydrate upon protein binding, especially those involving hydrogen bonding.

It is well known that the isotropic chemical shift is an important diagnostic tool in carbohydrate chemistry.[2] The hydroxyl proton chemical shift and its scalar coupling are most informative in studying hydrogen bonding; however, detection is often complicated by exchange phenomena.[3] Although skeleton carbon and proton chemical shift changes are less pronounced, they can be correlated with hydrogen bonding interactions,[4] and since these nuclei do not undergo exchange, their detection is simpler in aqueous solution. Moreover, the proton spectra of simple carbohydrates may show strong coupling effects and the resonances are often ill resolved. These factors combined make carbon detection an invaluable tool in carbohydrate research and for the work reported herein.

The chemical shift is a tensorial quantity with three principal components whose values can only be determined from solid-state NMR. The isotropic chemical shift is mathematically defined as the average of three principal components (δ_{11}, δ_{22}, and δ_{33}) which define the chemical shift tensor (shielding is expressed in parts per million (ppm) units), eq 1. It is well

$$\delta_0 = {}^1/_3(\delta_{11} + \delta_{22} + \delta_{33}) \tag{1}$$

documented that the shift tensor is extremely sensitive to bond length, geometry, and electronic features.[5] Isotropic chemical shift is often not a very sensitive parameter to subtle changes in local electronic structure because the principal components are averaged. In contrast, chemical shift anisotropy ($\Delta\delta$) (defined by eq 2) is a direct measure of the deviation of the

$$\begin{aligned} \Delta\delta &= {}^3/_2(\delta_{11} - \delta_0), \quad \text{when } |\delta_{11} - \delta_0| \geq |\delta_{33} - \delta_0| \\ \Delta\delta &= {}^3/_2(\delta_{33} - \delta_0), \quad \text{when } |\delta_{33} - \delta_0| \geq |\delta_{11} - \delta_0| \end{aligned} \tag{2}$$

principal components from their mean and may be more characteristic for structural changes.

Chemical shift anisotropy detection to measure electronic and geometrical behavior in large biomolecules is an area of increasing interest.[6] Single crystal CSA studies are promising because tensorial data are available from the NMR crystal structure.[7] However, crystal data are not always relevant to solution phenomena. Proton detected solution-phase ^{1}H CSA[8a]

† Presented in part at the 208th National Meeting of the American Chemical Society, Washington, DC, Aug 17−22, 1994.

‡ Permanent Address: Research Group for Antibiotics of the Hungarian Academy of Sciences L. Kossuth University, H-4010 Debrecen, P.O. Box 70, Hungary.

® Abstract published in *Advance ACS Abstracts*, December 1, 1994.

(1) For different examples see: Phillips, L. M.; Nudelman, E.; Federico C. A. Gaeta, Perez, M.; Singhal, A. K.; Hakomori, S.-I.; Paulson, J. C. *Science* **1990**, *250*, 1130. Walz, G.; Aruffo, A.; Kolanus, W.; Bevilacqua, M.; Seed, B. *Science* **1990**, *250*, 1132. Schonfeld, H.; Helwig, H. *Bacterial Meningitis*; Karger Publishers: New York, 1992.

(2) Bock, K.; Pedersen, C. *Adv. Carbohydr. Chem. Biochem.* **1983**, *41*, 27. Bock, K.; Pedersen, C.; Pedersen, H. *Adv. Carbohydr. Chem. Biochem.* **1983**, *41*, 193. Vliegenthart, J.; Dorland, L.; van Halbeck, H. *Adv. Carbohydr. Chem. Biochem.* **1983**, *41*, 209.

(3) Bock, K.; Lemieux, R. U. *Carbohydr. Res.* **1982**, *100*, 63. Poppe, L.; von der Lieth, C.-W.; Dabrowski, J. *J. Am. Chem. Soc.* **1990**, *112*, 7762. Ejchart, A.; Dabrowski, J.; von der Lieth, C.-W. *Magn. Reson. Chem.* **1992**, *30*, S-105. Poppe, L.; Stuike-Prill, R.; Meyer, B.; van Halbeck, H. *J. Biomol. NMR* **1992**, *2*, 109. Dabrowski, U.; Dabrowski, J.; Grosskurth, H.; von der Lieth, C.-W.; Ogawa, T. *Biochem. Biophys. Res. Commun.* **1993**, *192*, 1057. Adams, B.; Lerner, L. *Magn. Reson. Chem.* **1994**, *32(4)*, 225.

(4) Reuben, J. *J. Am. Chem. Soc.* **1984**, *106*, 6180. Christofides, J. C.; Davies, D. B.; Martin, J. A.; Rathbone, E. B. *J. Am. Chem. Soc.* **1986**, *100*, 5738. Hansen, P. E. *Progress in Nuclear Magnetic Resonance Spectroscopy* Emsley, J. W., Feeney, J., Sutcliffe, L. H., Eds; Pergamon Press: Oxford, 1988; p 30. Hansen, P. E.; Christoffersen, M.; Bolvig, S. *Magn. Reson. Chem.* **1993**, *31*, 893.

(5) Webb, G. A. In *Nuclear Magnetic Shieldings and Molecular Structure*; Tossell, J. A., Ed; Kluwer Academic Publishers: The Netherlands, 1993; p 1. Grimmer, A. R. *Ibid.* p 191.

(6) Mai, W.; Hu, W.; Wang, C.; Cross, T. A. *Protein Sci.* **1993**, *2*, 532. Searle, M. S.; Lane, A. N. *FEBS Lett.* **1992**, *297*, 292.

(7) Sherwood, M. H.; Alderman, D. M.; Grant, D. M. *J. Magn. Reson. A* **1993**, *104*, 132. Grant, D. M.; Facelli, J.; Alderman, D. W.; Sherwood, M. H. *Ibid.* **1993**, *104*, 367.

(8) (a) Werbelow, L. *J. Phys. Chem.* **1990**, *94*, 6663. (b) Poppe, L.; van Halbeek, H. *Magn. Reson. Chem.* **1993**, *31*, 665.

0002-7863/95/1517-0368$09.00/0

data for ^{13}C-enriched carbohydrates[8b] have been reported, and in lack of tensor data axial symmetry is invoked to determine the CSA values.[8,9]

We decided to explore the possibility of using carbon detected ^{13}C and ^{1}H CSA as a sensitive indicator of electronic changes occurring at carbon and proton nuclei proximal to hydroxyl groups possibly involved in hydrogen bonding. As we demonstrate herein, CSA can be easily measured outside the extreme narrowing regime, making this parameter particularly useful in studying macromolecular species.[10] Our NMR methods for detecting solution-phase ^{1}H and ^{13}C CSA in sialic acid **1** and its α-(2→8) linked homopolymer, colominic acid **2**, are

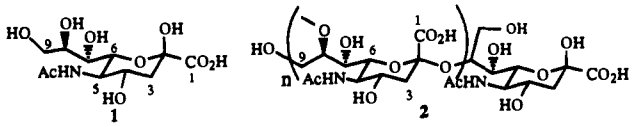

described. We also present the first liquid-phase CSA study on a polysaccharide and a comparison of monomer and polymer CSA data.

Theory

Proton and carbon chemical shift anisotropy relaxation is a weak process, usually masked by dipole−dipole relaxation (DD), and generally it is not straightforward to extract its contribution to the overall relaxation of a nucleus. In a C−H two-spin system, dipolar relaxation occurs by the magnetic moment of one nucleus creating a magnetic field at the other spin. CSA relaxation involves only one spin and depends on the anisotropic electronic environment of the nucleus. As the molecule tumbles, the local field at the nucleus varies which causes the spin to relax. If these two relaxation mechanisms (CSA and DD) are cross-correlated,[11] then in an inversion recovery experiment the two lines of the C−H doublet relax at different rates, giving rise to an asymmetric doublet or two-spin order formation.[12]

Several experiments have been developed which allow the interference of CSA relaxation with dipolar relaxation to be measured, including DQ-filtered inversion recovery,[13] polarization transfer,[14,15] two-dimensional soft NOESY,[16] DQF-NOESY,[17] ortho-ROESY,[18] SLOESY,[19] and Overbodenhausen inverse experiments.[20] There are only a few examples of quantitative CSA studies occurring in the literature where

DQ-Filtered Transient NOE

Phase Cycling for Difference:	Φ1=	x	-x	x	-x	x	-x	x	-x
	Φ2=	y	y	-y	-y	-y	-y	y	y
	Φ3=	x	x	-x	-x	-x	-x	x	x
	Φ4=	x	x	x	x	-x	-x	-x	-x
	Φ5=	x	x	x	x	-x	-x	-x	-x
Phase Cycling for Reference:	Φ2=	y	y	y	y	-y	-y	-y	-y
	Φ3=	x	x	x	x	-x	-x	-x	-x
	Φ4=	-x	-x	-x	-x	x	x	x	x

Figure 1. The DQ-filtered transient heteronuclear NOE pulse sequence for determination of ^{1}H CSA_g. *Thin* bars represent 90° and *thick* bars 180° pulses.

isotopic labeling is not employed.[15,21] Natural abundance CSA detection experiments require special consideration. The sensitivity gain normally associated with inverse experiments is sometimes difficult to achieve at natural abundance owing to practical difficulties in eliminating ^{12}C attached ^{1}H magnetization. We investigated several different approaches and, for the purposes of natural abundance ^{1}H and ^{13}C CSA measurements, we modified some of the aforementioned techniques.

In this work we measure the relaxation mediated conversion of longitudinal magnetization $\langle S_Z \rangle$ into heteronuclear two-spin order $\langle 2S_Z I_Z \rangle$ and vice versa.[22] Quantitative evaluation of the resulting spectral densities yields information about the CSA tensor, giving structural information which is difficult to obtain in the liquid state by other means.

Proton CSA Methods

For carbon detected ^{1}H CSA measurements, we implemented a double-quantum filtered[13] transient NOE[9a] experiment. The pulse sequence begins with ^{1}H inversion which is followed by a free evolution period to allow the buildup of heteronuclear two-spin order. The two-spin order $\langle 2I_Z S_Z \rangle$ is then converted to $\langle 2I_Y S_X \rangle$ coherence which is transformed to observable antiphase ^{13}C magnetization by the last ^{1}H pulse (Figure 1). Suppression of the natural ^{13}C signals is achieved by the simultaneous phase inversion of this read pulse and the receiver reference. In addition, phase alternation of the second ^{1}H pulse was applied with constant receiver phase to have difference spectra less dependent on pulse imperfections.

To obtain the equilibrium ^{13}C magnetization, the "reference" phase cycle in Figure 1, which is identical with a transient NOE experiment with zero mixing time ($\tau = 0$), was applied. The

(9) (a) Batta, Gy. 34th Experimental Nuclear Magnetic Resonance Conference, March 14−18, 1993, St. Louis, MO; P 18. (b) Batta, Gy.; Kover, K. E.; Gervay, J. 15th German NMR Conference, Friedrichroda, Sept 30, 1993. (c) Batta, Gy.; Kover, K. E.; Gervay, J. 35th Experimental Nuclear Magnetic Resonance Conference, April 10−15, 1994, Asilomar, CA; Abstract WP 40.

(10) Daye, K. T.; Zhang, P. L.; Wagner, G. 35th Experimental Nuclear Magnetic Resonance Conference, April 10−15, 1994, Asilomar, CA; Abstract MP 57. Brown, R. A.; Mayne, C. L.; Grant, D. M. *Ibid.*, Abstract WP 149.

(11) Shimizu, H. J. *J. Chem. Phys.* **1964**, *40*, 3357. Mackor, E. L.; Maclean, C. *J. Chem. Phys.* **1966**, *44*, 64. Werbelow, L. G.; Grant, D. M. *Adv. Magn. Reson.* **1977**, *9*, 189. Vold, R. L.; Vold, R. R. *Progr. NMR Spectrosc.* **1978**, *12*, 79. Goldman, M. *J. Magn. Reson.* **1984**, *60*, 437. Keeler, J.; Sánchez-Ferrando *J. Magn. Reson.* **1987**, *75*, 96. Canet, D. *Prog. NMR Spectrosc.* **1989**, *21*, 237. Grant, D. M.; Mayne, C. L.; Liu, F.; Xiang, T. X. *Chem. Rev.* **1991**, *91*, 1591.

(12) Guéron, M.; Leroy, J. L.; Griffey, R. H. *J. Am. Chem. Soc.* **1983**, *105*, 7262.

(13) Jaccard, G.; Wimperis, S.; Bodenhausen, G. *Chem. Phys. Lett.* **1987**, *138*, 601.

(14) (a) Tsai, C.-L.; Price, W. S.; Chang, Y.-C.; Perng, B.-C.; Hwang, L.-P. *J. Phys. Chem.* **1990**, *95*, 7546. (b) Trudeau, J. D.; Bohmann, J.; Farrar, T. C. *J. Magn. Reson. A* **1993**, *105*, 151. (c) Farrar, T. C.; Jablonsky, M. J.; Schwartz, J. L. *J. Phys. Chem.* **1994**, *98*, 6244.

(15) Chang, W.-T.; Wang, P.-L.; Duh, D.-M.; Hwang, L.-P. *J. Phys. Chem.* **1990**, *94*, 1343.

(16) (a) Oschkinat, H.; Clore, G. M.; Gronenborn, A. M. *J. Magn. Reson.* **1988**, *78*, 371. (b) Oschkinat, H.; Bermel, W. *J. Magn. Reson.* **1989**, *81*, 220. (c) DiBari, L.; Kowalewski, J.; Bodenhausen, G. *J. Chem. Phys.* **1990**, *93*, 7698.

(17) (a) Dalvit, C.; Bodenhausen, G. *Chem. Phys. Lett.* **1989**, *161*, 554. (b) Dalvit, C. *J. Magn. Reson.* **1991**, *95*, 410.

(18) Bruschweiler, R.; Ernst, R. R. *J. Chem. Phys.* **1992**, *96*, 1758.

(19) (a) Bull, T. E. *J. Magn. Reson.* **1988**, *80*, 470. (b) Burghardt, I.; Konrat, R.; Bodenhausen, G. *Mol. Phys.* **1992**, *75*, 467.

(20) Boyd, J.; Hommel, U.; Campbell, I. D. *Chem. Phys. Lett.* **1990**, *175*, 477.

(21) (a) Farrar, T. C.; Jablonski, M. J. *J. Phys. Chem.* **1991**, *95*, 9159. (b) Kontaxis, G.; Muller, N.; Sterk, H. *J. Magn. Reson.* **1991**, *92*, 332. (c) Zheng, Z.; Mayne, C. L.; Grant, D. M. *J. Magn. Reson. A* **1993**, *103*, 268. (d) Maler, L.; Kowalewski, J. *Chem. Phys. Lett.* **1992**, *192*, 595. (e) Maler, L.; Di Bari, L.; Kowalewski, J. *J. Phys. Chem.* **1994**, *98*, 6244.

(22) Transverse magnetization transfer can also be used but was not considered in this work.

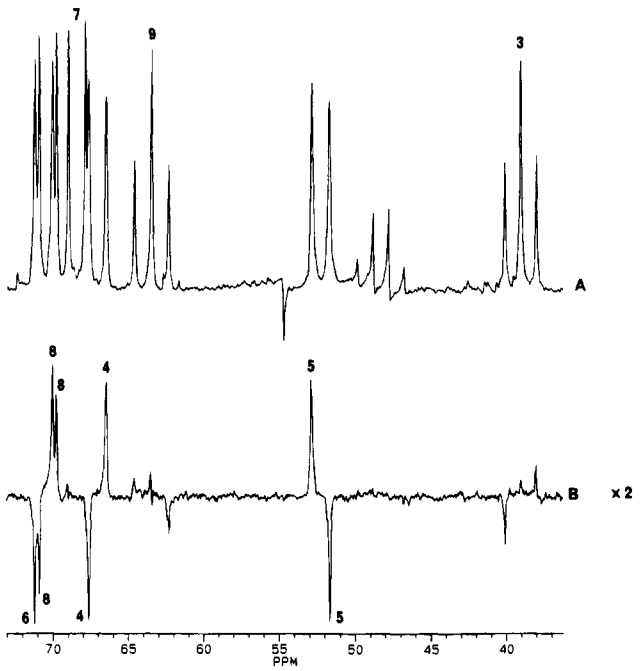

Figure 2. ^{1}H CSA_g difference spectrum of 0.9 M sialic acid (B) with reference spectrum (A); 256 transients were accumulated in each experiment (delay = 0.25 s). The NHAc signal is a folded quartet in spectrum A.

equilibrium ^{1}H magnetization is derived by multiplying the ^{13}C magnetization by the ratio of gyromagnetic factors γ(H)/γ(C). The initial buildup rate (eq 3) of the antiphase ^{13}C doublet,

$$\delta_{SIS} = \frac{\langle 2S_Z I_Z \rangle}{2 < S_{Z^0} > dt} \tag{3}$$

referenced to the double ^{1}H intensity,[23] is proportional to the J_{SIS} spectral density; hence the CSA contribution can be determined according to eq 4. Where J_{SIS} is the CSA/DD cross-

$$J_{SIS}(\omega_S) = \frac{1}{10}\frac{\mu_0}{4\pi}\gamma_S^2\gamma_I\hbar\langle r_{IS}^{-3}\rangle B_0 \Delta\sigma_S \left[\frac{\tau_C}{1+\omega_S^2\tau_C^2}\right] \times \underbrace{[^1/_2(3\cos^2\Phi_{SIS} - 1)]}_{\text{geometric term}} \tag{4}$$

correlated spectral density and $\Delta\sigma_S$ is the chemical shielding anisotropy of nucleus S which in this case is hydrogen. The angle subtended by the C,H vector and the CSA symmetry axis is labeled Φ. This angle cannot be separated from $\Delta\sigma_S$ in solution phase,[24] therefore, we arbitrarily set a parallel C,H vector and CSA symmetry axis making $\Phi = 0$ which gives a

(23) Equation 3 is an initial rate solution of the generalized two-spin Solomon equations.

$$d(v)/dt = -Rv(t) \tag{3a}$$

where

$$v = \begin{pmatrix} \langle S_Z \rangle \\ \langle I_Z \rangle \\ \langle 2S_Z I_Z \rangle \end{pmatrix} \quad \text{and} \quad R = \begin{pmatrix} \varrho_S & \sigma_{IS} & \delta_{SIS} \\ \sigma_{IS} & \varrho_I & \delta_{SII} \\ \delta_{SIS} & \delta_{SII} & \varrho_{IS} \end{pmatrix}$$

The general solution of these coupled linear differential equations is triple exponential for any of the three observable longitudinal magnetizations. However, we show in the Discussion that for our experiments double exponential fits are sufficient.

(24) Wagner, G. 35th Experimental NMR Conference, April 10–15, 1994, Asilomar, CA, T am 11:35, p 50.

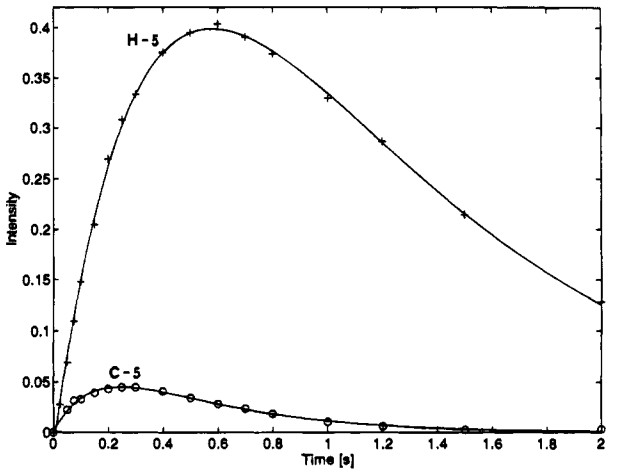

Figure 3. DQF–NOE buildup curve for H5 CSA_g and polarization transfer buildup curve (pulse sequence is shown in Figure 6) for C5 CSA_g in sialic acid.

value of 1 for the geometric term. Because we make the assumption of axial symmetry, we now introduce a new geometry dependent CSA_g parameter which is obtained by normalizing the geometric term in eq 4 and is defined by eq 5.

$$CSA_g = -\frac{40\pi}{\mu_0 B_0}\frac{J_{SIS}(\omega_S)}{\gamma_S^2\gamma_I\hbar}\frac{1}{\langle r_{IS}^{-3}\rangle}\frac{1+\omega_S^2\tau_C^2}{\tau_C}10^6 \tag{5}$$

The transient ^{13}C-{^{1}H} NOE is as much as 100% depending on the motional regime. However, the overall sensitivity of the two-spin order detection arises primarily from the sizable inverted ^{1}H magnetization. Figure 2 shows the carbon detected ^{1}H CSA difference spectrum (τ = 0.5 s delay) along with the reference spectrum obtained for a 0.9 M solution of sialic acid **1** in D_2O (11.76 T, 10-mm diameter sample, 274 K, pH 1).[25] It is interesting to note that the phase of the C5 antiphase doublet is opposite to that of the other signals, indicating a positive H5 CSA. The buildup curve shown in Figure 3 was generated using different variable delay values and fit with a double exponential function[26] to determine the initial rate of two-spin order formation. The conversion rate δ_{SIS} is proportional to the cross-correlated spectral density J_{SIS} as shown in eq 6.

$$\delta_{SIS} = -4J_{SIS}(\omega_S) \tag{6}$$

There are two simple methods with which the correlation time τ_C can be measured.[27] The C/H cross-relaxation rate can be determined either directly from transient NOE buildup (with

(25) The carbon chemical shifts were unambiguously assigned using COSY and HETCOR experiments: Gervay, J.; Batta, Gy. *Tetrahedron Lett.* **1994**, *35*, 3009.

(26) MATLAB 4.1.1, Optimization Toolbox, Mathworks, Natick, MA, 1993. We note that the transient NOE buildup curves could always be fitted with triple exponential curves.

(27) (a) We considered the model free approach,[27b–d] and a hybrid method was attempted in which we input a fixed global correlation time for the model free iteration routine. The global correlation time was obtained by averaging the local correlation times obtained by the cross-relaxation method. Most of the CSA_g data obtained with this method were in quantitative agreement with the values we report and the qualitative trends were also comparable. This agreement can partly be explained by an ordered structure where the internal motions are reduced and the local correlation times approach the value of the molecular correlation time. In fact, the temperature of these experiments was chosen in order to diminish the role of internal motions as well as to maximize chemical stability and to enhance the sensitivity. (b) Dellwo, M. J.; Wand, A. J. *J. Am. Chem. Soc.* **1989**, *111*, 4571. (c) Lipari, G.; Szabo, A. *J. Am. Chem. Soc.* **1982**, *104*, 4546. (d) Lipari, G.; Szabo, A. *J. Am. Chem. Soc.* **1982**, *104*, 4559.

Table 1. Spectral Data for Sialic Acid 0.9 M in D_2O at 274 K

	δ^a (ppm)	C T_1 (s)	NOEF	τ_c ($\times 10^{-10}$ s)	$\delta_{SII}{}^b$ (Hz)	^{13}C CSA$_g$ (ppm)	$\delta_{SIS}{}^b$ (Hz)	^{1}H CSA$_g$ (ppm)
C4	67.0	0.256	0.659	5.87	0.306	14.8	−0.237	−10.5
C5	52.3	0.246	0.687	5.35	0.500	25.7	0.248	10.4
C6	70.6	0.252	0.674	5.61	0.659	32.9	−0.232	−10.0
C7	68.4	0.251	0.584	6.54	0.638	28.9	0	0
C8	70.3	0.269	0.626	6.54	0.373	16.9	−0.162	−7.6
C9	63.6	0.167	0.781	6.51				

[a] Relative to dioxane external standard. [b] $\langle 2I_ZS_Z\rangle$ to $\langle S_Z\rangle$ or $\langle S_Z\rangle$ to $\langle 2I_ZS_Z\rangle$ conversion rates. τ_c is the isotropic correlation time.

^{1}H decoupling during acquisition) or from eq 7,[28] where T_1 is

$$\sigma_{IS} = \frac{\gamma_I}{\gamma_S}\frac{\mathrm{NOEF}}{T_1} \tag{7}$$

the ^{13}C spin−lattice relaxation time and NOEF is the ^{13}C-{^{1}H} NOE factor under broad band ^{1}H decoupling. The cross-relaxation rate gives τ_C from eq 8.

$$\sigma_{IS} = \frac{1}{10}K^2\tau_C\left[\frac{6}{1+(\omega_I+\omega_S)^2\tau_C{}^2} - \frac{1}{1+(\omega_I-\omega_S)^2\tau_C{}^2}\right] \tag{8}$$

$$K = (\mu_0/4\pi)\hbar\gamma_I\gamma_S r_{IS}{}^{-3} \qquad (r_{IS} = 1.12\ \text{Å})$$

We found the latter method to be more accurate since CSA and other competing relaxation mechanisms are inherently considered in eq 7; moreover, the transient NOE is smaller than the steady-state NOEF. The values for the cross-correlated relaxation rates and correlation times in a 0.9 M solution of sialic acid are given in Table 1. The CSA$_g$ values listed in Table 1 were calculated using eqs 5 and 6 assuming axial symmetry. An identical procedure was used to obtain the data for colominic acid (**2**). A representative DQF−NOE difference spectrum of 0.03 M colominic acid in D_2O (11.76 T, 10-mm diameter sample, 299 K, pH 7) is shown in Figure 4. The colominic acid buildup curve is shown in Figure 5. The results of these experiments are shown in Table 2.

Carbon CSA Methods

Liquid-phase ^{13}C CSA$_g$ data can be obtained from DQ-filtered ^{13}C inversion recovery experiments; however, at natural abundance sensitivity remains a problem. A plausible solution to insensitivity is to use a refocussed INEPT[29] sequence to prepare the ^{13}C spins. In fact, the INEPT sequence yields the expected enhancement, but there is considerable data scattering in the initial buildup period presumably caused by incomplete refocussing. Instead, we significantly modified the polarization transfer sequence of Hwang.[15] Our version is shown in Figure 6. Development of antiphase ^{1}H magnetization is allowed with ^{13}C chemical shift refocussing; then a random duration spin lock field is applied scan by scan to filter out unwanted in-phase ^{1}H magnetization. The resulting pure antiphase signal is converted to two-spin order by a proton pulse polarizing the ^{13}C transitions at the same time. While the two ^{13}C transitions of the CH group are equally polarized, they are affected differently by CSA/DD cross-correlated relaxation during the delay τ, resulting in different line intensities after the final read pulse. This difference can be conveniently measured by switching on the decoupler during acquisition and quenching the antiphase part of the signal, after which only one-spin order $\langle I_Z\rangle$ survives. The resulting buildup curve shows the formation of $\langle I_Z\rangle$ from two-spin order $\langle 2S_ZI_Z\rangle$. The reference experiment is a refocussed INEPT, which contains an extra $1/(2J)$ refocussing delay. However, no significant amount of ^{13}C magnetization is lost

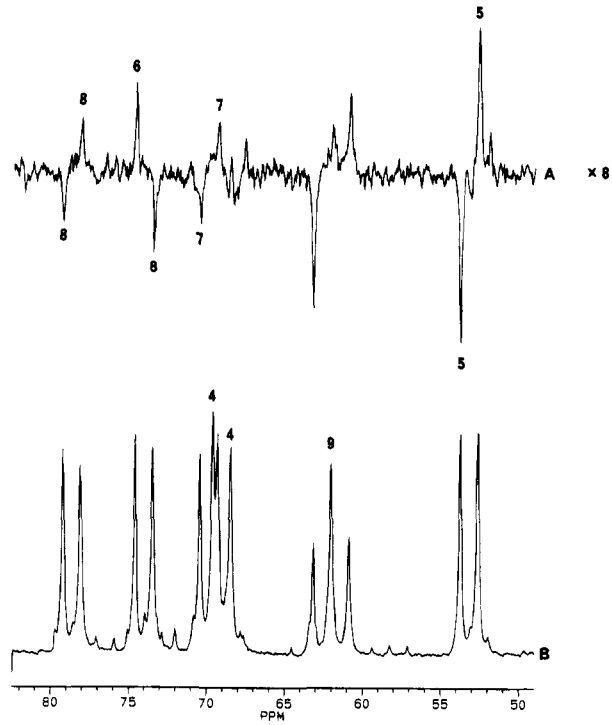

Figure 4. ^{1}H CSA$_g$ difference spectrum of colominic acid (A) with reference spectrum (B); 1504 transients were accumulated for each spectrum (delay = 0.8 s).

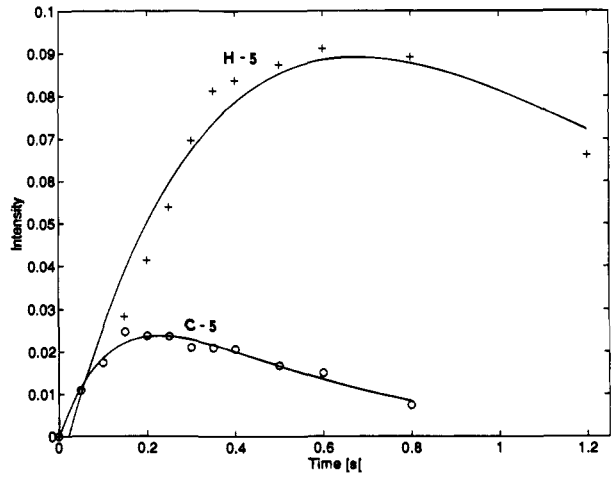

Figure 5. DQF−NOE buildup curve for H5 CSA$_g$ and polarization transfer buildup curve (pulse sequence is shown in Figure 6) for C5 CSA$_g$ in colominic acid.

Table 2. Spectral Data for Colominic Acid 0.03 M in D_2O at 299 K

	δ^a (ppm)	C T_1 (s)	NOEF	τ_c ($\times 10^{-10}$ s)	$\delta_{SII}{}^b$ (Hz)	^{13}C CSA$_g$ (ppm)	$\delta_{SIS}{}^b$ (Hz)	^{1}H CSA$_g$ (ppm)
C4	68.9	0.407	0.364	17.0	0.270	10.4	0	0
C5	52.9	0.381	0.374	15.5	0.300	11.3	−0.050	−4.7
C6	73.8	0.381	0.360	16.1	0.356	13.5	0.033	3.2
C7	69.3	0.418	0.352	18.0	0.419	16.5	−0.016	−1.7
C8	78.7	0.384	0.371	15.7	0.415	15.7	−0.018	−1.7
C9	61.8	0.167	0.486	10.5				

[a] Relative to dioxane external standard. [b] $\langle 2I_ZS_Z\rangle$ to $\langle S_Z\rangle$ or $\langle S_Z\rangle$ to $\langle 2I_ZS_Z\rangle$ conversion rates. τ_c is the isotropic correlation time.

(28) Neuhaus, D.; Williamson, M. *The Nuclear Overhauser Effect in Structural and Conformational Analysis*; VCH Publishers: New York, 1989.
(29) Morris, G.; Freeman, R. *J. Am. Chem. Soc.* **1979**, *101*, 760.

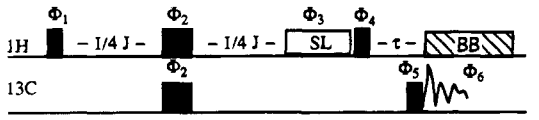

Polarization Transfer

Phase Cycling:								
Φ1=	x	x	x	x	x	x	x	x
Φ2=	x	-x	x	-x	x	-x	x	-x
Φ3=	x	x	x	x	x	x	x	x
Φ4=	y	y	-y	-y	-y	-y	y	y
Φ5=	y	y	-y	-y	y	y	-y	-y
Φ6=	y	y	y	y	-y	-y	-y	-y

Figure 6. Polarization transfer pulse sequence for monitoring ^{13}C CSA_g. J is the one-bond coupling constant, the spin lock time is 3 ms with 50% random variation, and τ is the variable delay.

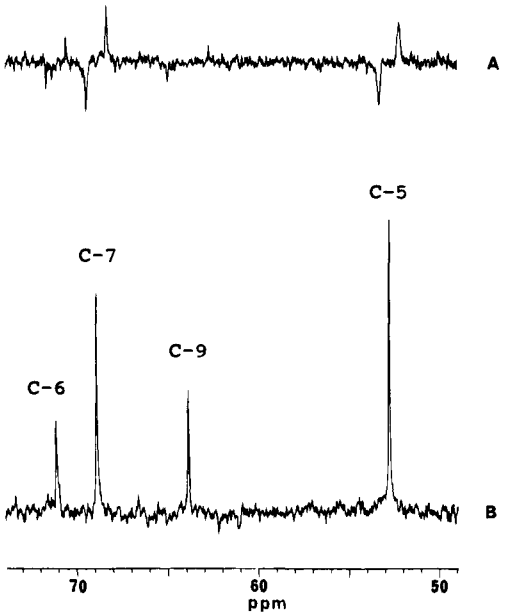

Figure 7. Carbon detected difference spectrum for ^{13}C CSA_g determination of sialic acid at 299 K (768 transients, $\tau = 0.6$ s). Spectrum A is from a conventional DQF-inversion recovery sequence and spectrum B is obtained by the polarization transfer method shown in Figure 6. A sensitivity gain of ca. 6 is obtained by method B.

during this period because the ^{13}C T2 range is on the order of 100-ms scale which is long compared to the 3.4-ms delay for the $1/(2J)$ period. Application of the same delays in the ^{13}C CSA experiment and the reference INEPT along with the uniformity of the carbohydrate one bond C,H couplings makes the referencing errors small compared to the detection of two-spin order. It should be pointed out that sign information is lost; however, this information can be retrieved from a single INEPT enhanced double-quantum filtered inverstion recovery experiment.

The new polarization transfer difference spectrum of a 0.9 M solution of sialic acid compared to a conventional DQF-inversion recovery experiment[30] (both having equal transients) is shown in Figure 7. The maximum signal-to-noise ratio enhancement expected was 8, and an enhancement of approximately 6 was realized. The polarization transfer and the conventional (reference) broad band decoupled ^{13}C spectra of 0.03 M colominic acid are shown in Figure 8. The polarization transfer buildup curves for ^{13}C-CSA_g were fit with double exponential functions to provide the initial rate for relaxation

(30) The DQF-inversion recovery experiment gave similar values for the conversion rate, but the error limits were higher.

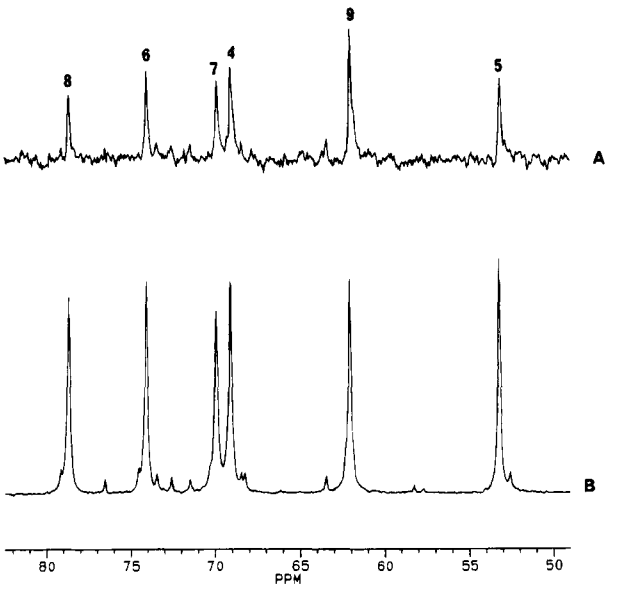

Figure 8. Spectrum A is the polarization transfer (Figure 6) spectrum for ^{13}C CSA_g determination of colominic acid. Spectrum B is a regular proton decoupled ^{13}C spectrum. The small peaks on spectrum B are due to inhomogeneity of the polymer.

rates δ_{SII}. The data for sialic acid are listed in Table 1 and those for colominic acid are in Table 2.

Discussion

It is worthwhile to comment on the experimental finding that the two-spin order buildup curves for both the ^1H and ^{13}C CSA experiments could be adequately fitted with double exponential functions, while the transient NOE buildup required the expected triple exponential fit. In the DQF–NOE experiment, according to the difference experiment, the in-phase part of the carbon $\langle Z \rangle$ magnetization is filtered out. The effect of cross-relaxation (σ_{IS}) is eliminated since cross-relaxation always results in the formation of net $\langle Z \rangle$ magnetization. On the other hand, the initial preparation (^1H inversion) allows only the conversion of ^1H $\langle Z \rangle$ magnetization to two-spin order. Carbon $\langle Z \rangle$ magnetization may be formed in multistep relaxation processes from two-spin order; however, this is a weak process. If we consider the change of two-spin order in eq 3a,[23] we find that $\langle I_Z \rangle$ is cancelled. The two-spin order formation rate is governed by the cross-correlated rate δ_{SIS}, and its decay is determined by its intrinsic relaxation rate δ_{IS}. Similar qualitative considerations suggest that the buildup curves in the ^{13}C CSA experiments may also be adequately fit with double exponential functions.

Theoretical density matrix calculations have recently been applied by Farrar and co-workers for description of related experiments.[14b] Following their numerical method we were able to simulate and fit our data. The DQF–NOE experiment (Figure 1) is generated from a transient NOE experiment taking the difference between the two carbon lines. In the polarization transfer experiment (Figure 6), we obtain two different forms of the analogous "pure J-state" experiment for the ^{13}C CSA determination. Broadband ^1H decoupling was simulated by coaddition of lines, and the difference is calculated according to the given phase program. Using this approach we fit all C,H pairs of sialic acid (e.g., the pair in Figure 3) separately. The known correlation times were fixed and the curve pairs were fitted for the A,B random relaxation contributions and the ^1H and ^{13}C CSA values. We found that all curve pairs could be well fitted by the density matrix method, and the resulting CSA values differed only by 4–6% from the values obtained by the

initial rate method. Moreover, the theoretical points obtained by the density matrix approach could easily be fitted with double exponential functions. The A,B random field contributions were in the range of 1 Hz; however, in some cases the proton term was negative. The origin of this is not clear, but may be due to either multispin effects, which are more pronounced for protons, or to unidentified solvent interactions. Fortunately, neither the initial rates nor the CSA_g values are sensitive to the random field contributions.

By definition the CSA_g values compiled in Tables 1 and 2 represent lower limits for the absolute value of CSA ($|\Delta\sigma_S|$) since the geometrical factor can have a value between 1 and $-1/2$. Although we arbitrarily set $\phi = 0$, it is possible that the tensor axis is not parallel with the CH vector in which case the geometrical factor would have a value less than 1. Since $|\Delta\sigma_S|$ is inversely proportional to the geometrical factor, it would necessarily be larger for any other value of ϕ. The sign of CSA_g is determined by both $\Delta\sigma_S$ and the geometrical factor simultaneously. If they are the same sign, CSA_g is negative; if they are opposite in sign, CSA_g is positive. The sign of $\Delta\sigma_S$ depends upon the values of the principal components (eq 2) and is very sensitive to small changes. The sign of the geometrical factor is determined by the angle ϕ which changes sign at the magic angle of approximately 55°. In these studies we cannot determine if the sign arises from $\Delta\sigma_S$ or ϕ because these quantities cannot be measured independently.

The ^{13}C CSA_g values are all positive for both sialic acid and colominic acid. The largest difference in ^{13}C CSA_g is at C6 ($\Delta CSA_g = {}^{13}C\text{-}CSA_{SA} - {}^{13}C\text{-}CSA_{CA}$) with ΔCSA_g, C6 = 19.4 ppm. Carbons 5 and 7 also show large changes (ΔCSA_g = 14.4 and 12.4 ppm, respectively), whereas C4 and C8 are less affected (ΔCSA_g = 4.4 and 1.2 ppm, respectively). If ϕ is the same for similar carbons in the monomer and polymer, differences in CSA_g values may reflect differences in shielding of the principal component relative to the isotropic chemical shift. Our results show that, in so far as the geometric factor is greater than 0 and is similar for the same carbon atoms, the "parallel" principal components in sialic acid from C4 to C7 are deshielded if compared to the polymer. Position C8 is an exception, perhaps because this is the site of glycosylation. The "orthogonal" components are all more shielded in the monomer, in so far as the tensors are axially symmetric. This finding may result from the tertiary structure of the polymer and/or differences in solvation. The polymer may exclude solvent molecules, whereas sialic acid is believed to be highly solvated in water. The impact of hydrogen bond formation on carbon chemical shift anisotropy is not yet resolved.

Similar to ^{13}C CSA_g trends, the ^{1}H CSA_g values are generally smaller in the polymer. The changes in ^{1}H CSA_g were again largest for H5 and H6 (15.1 and −13.2 ppm, respectively); however, H4 and H8 also showed large differences (−10.5 and −5.9 ppm, respectively).[31] We were unable to detect ^{1}H CSA_g for either H7 in sialic acid or H4 in colominic acid. It is possible that ϕ is close to 55° for these nuclei, in which case the geometric term becomes 0 as does the spectral density according to eq 4. It is predictable that proton shift anisotropies are quite

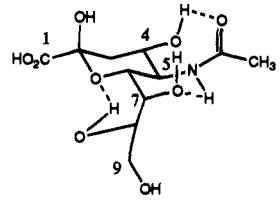

Figure 9. Intramolecular hydrogen bonding in sialic acid.

sensitive to solvent effects; however, further studies are required before a clear connection between proton CSA_g values of CH groups and neighboring hydroxyl hydrogen bonding can be correlated.

Thornton and co-workers reported ^{13}C spin−lattice relaxation data for 0.68 M solutions of sialic acid in D_2O at 28 °C.[32] They showed that the correlation time τ_C for the C7 and C8 carbons were similar (1.8×10^{-10} s) to the pyranose carbons suggesting that the motions of C7 and C8 were concerted with the ring. In contrast, C9 showed increased mobility relative to the pyranose as indicated by a $\tau_C = 1.1 \times 10^{-10}$ s. These data provided evidence of intramolecular hydrogen bonding between the C7, C8 hydroxyls and the pyranose ring as shown in Figure 9.[33] Our correlation times (Table 1) indicate that the glycerol side chain motions are similar ($\tau_C \sim 6.5 \times 10^{-10}$ s) and slower than those of the pyranose ring ($\tau_C \sim 5.6 \times 10^{-10}$ s) making strong intramolecular hydrogen bonding less likely.[34] However, it is possible that the glycerol side chain is involved in *intermolecular* hydrogen bonding interactions which restrict its motion relative to the pyranose ring. In fact, sialic acid is known to crystallize in two different forms: a dehydrated form involving intramolecular hydrogen bonding,[35] similar to that proposed by Thornton, and a hydrated form where intermolecular hydrogen bonding to water is observed.[36] Dilution studies combined with relaxation data may give more information about the hydrogen bonding network, but such studies are outside of the scope of this work.

The local correlation times for colominic acid are shown in Table 2. As expected the polymer motions are slower than in the monomer, even at increased temperature. In colominic acid, the C7 and C8 motions are similar to the pyranose ring ($\tau_C \sim 16 \times 10^{-10}$ s), whereas C9 ($\tau_C \sim 11 \times 10^{-10}$ s) is more freely rotating in contrast to the concerted side-chain motion in sialic acid. Differences in the side-chain conformations of sialic acid and colominic acid have been reported.[37] Coupling constant data indicate that the glycerol chain conformation about the C8/C7 and C7/C6 bonds is anti/gauche[38] in sialic acid and gauche, gauche in colominic acid.[39]

The studies thus far clearly show that pronounced conformational changes occur in polymers of α-(2→8) linked sialic acid relative to the monomer. Concomitant changes in hydrogen bonding must also occur; however, hydrogen bonding phenomena in these systems are much less understood. The ^{1}H and ^{13}C CSA_g data, while preliminary, are consistent with earlier

(31) (a) During the review process it was suggested that the measurements indicating unusually large proton CSA values may be invalidated by three spin effects. Grant[32b] provided experimental evidence that the initial rate approximation is free from multispin effects in his work on ethanol. Additionally, we obtained very good fits with the initial rate from both double-exponential and density matrix methods. Since the density matrix method is exact for two-spins, the agreement suggests that multispin effects do not interfere with the initial rate method. The least significant digits in the CSA_g numerical values result from their derivation without round-off errors. The estimated errors of the CSA values for sialic acid are ±10% and those for colominic acid are ±30%. (b) Zheng, Z.; Mayne, C. L.; Grant, D. M. *J. Magn. Reson. Ser. A* **1993**, *103*, 268.

(32) Czarneicki, M.; Thornton, E. R. *J. Am. Chem. Soc.* **1976**, *98*, 1023.

(33) There has been some suggestion that the difference between these correlation times is not large enough to be considered significant: Sabesan, S.; Bock, K.; Lemieux, R. U. *Can. J. Chem.* **1984**, *62*, 1034 and references therein.

(34) We believe that the difference in these correlation times is significant because there was very little scatter in the data and these values lie outside the error limits.

(35) Ogura, H.; Furuhata, K.; Saito, H.; Izumi, G.; Itoh, M.; Shitori, Y. *Chem. Lett.* **1984**, 1003.

(36) Flippen, J. L. *Acta Crystallogr., Sect. B* **1973**, *29*, 1881.

(37) Michon, F.; Brisson, J.-R.; Jennings, H. J. *Biochemistry* **1987**, *26*, 8399.

(38) Brown, E. B.; Brey, W. S., Jr.; Weltner, W., Jr. *Biochim. Biophys. Acta* **1975**, *399*, 124.

(39) Yamasaki, R.; Bacon, B. *Biochemistry* **1991**, *30*, 851.

studies in that large effects at nuclei involved in both conformational and/or hydrogen bonding changes are observed; however, a simple interpretation of anisotropy cannot be given at this time.

Conclusion

In conclusion we have presented simple and sensitive NMR methods for detecting carbohydrate ^1H and ^{13}C CSA in concentrated aqueous solutions at natural abundance. The values obtained are in complete agreement with data from other pulse sequences used to determine CSA values for isotopically enriched carbohydrates. Large changes in ^1H and ^{13}C CSA_g values were observed for nuclei undergoing both conformational and/or hydrogen bonding changes presenting the possibility that CSA_g may be a sensitive parameter for monitoring these changes.

Investigations are continuing in our laboratory with simple monosaccharides in an effort to more clearly define how structural changes affect CSA_g values. Perhaps, quantum-chemical calculations would provide additional understanding.

Experimental Section

Sialic acid (0.9 M D_2O solution, pH 1) was prepared according to the method of Whitesides.[40] Colominic acid sodium salt obtained from *E. coli* (C 5762) was purchased from Sigma (St. Louis, USA) and was dissolved in D_2O to give 0.03 M solutions; the average polymer length was 30−35 monomer units. Both compounds were measured in 10-mm NMR tubes using 2 mL solutions. Oxygen depletion of the samples was not necessary because of exclusive carbon detection and relatively fast T_1 and T_2 relaxation's. Bruker AM-500 and 250 spectrometers were used with a VT 1000 temperature controller. Temperatures were calibrated either with 100% methanol (below 300 K) or ethylene glycol. The accuracy of temperature calibration is ±2 K, and the reproducibility is believed to be ±1 K.

The published data were obtained at 274 K for sialic acid because significant decomposition was observed at higher temperatures and the extreme broadening regime provided a more suitable correlation time. The higher molecular weight and chemical stability of colominic acid allowed observation at higher temperatures (299 K). Colominic acid was stable up to a month at this temperature.

^{13}C T_1 values were obtained with standard inversion recovery experiments using a 20−25 item variable delay list. Generally 10 T_1 relaxation delays were allowed before the inversion pulse. Typically 16−32 scans were accumulated for each point; the FIDs were weighted with matched exponential functions and zero filled. After Fourier transformation automatic, fourth order polynomial baseline correction was applied to the spectra. The inversion recovery curves were evaluated using a three-parameter single-exponential fit. Spectrometer built-in routines gave identical values for T_1 as a MATLAB application. For generating the ^{13}C-{^1H} NOEF values, the total number of scans of the difference experiment were comparable to the total number of scans in the T_1 experiments. The processing was done as for T_1 spectra, and the magnitudes of difference signals were compared to the reference spectrum. The accuracy of T_1 values was typically better than 2% and the relative error of the NOEF is less than 4%. The cross-relaxation rate of C−H vectors was obtained using eq 6, and the isotropic correlation time was calculated using eq 7. Cross-relaxation rates were also determined directly, in some cases, by monitoring the buildup rate of carbon magnetization following the inversion of proton magnetization's.

^1H CSA_g measurements were carried out using the DQF transient heteronuclear NOE sequence shown in Figure 1; 12−18 variable delays were used ranging from 0 to 2−5 ^{13}C T_1 values. A relaxation delay of 10 ^{13}C T_1 was allowed between pulse trains. In overnight experiments, typically 256−1600 scans were accumulated for each point. For ^{13}C CSA_g measurements the pulse sequence in Figure 6 was employed. The INEPT $1/(4J)$ delay was set according to an average 142-Hz one-bond coupling. The random ^1H spin lock field was applied at full power for 3 ms with ±50% randomization. Composite ^1H decoupling was applied at the lowest possible power during acquisition. Other parameters were similar to ^1H CSA_g experiments. The 90° ^{13}C and ^1H pulses for the 10-mm probe head at 11.76 T were 13 and 44 μs, respectively.

The cross-correlated relaxation rates were determined from the initial slope of the buildup curves after a double-exponential fitting of the entire curve. The analytical first derivative at zero delay gave the buildup rate. All calculations were carried out using the MATLAB software package.

Acknowledgment is made to the donors of the Petroleum Research Fund, administered by the American Chemical Society, and The State of Arizona Materials Characterization Program for partial support of this research. Gy. B. gratefully acknowledges the Hungarian Grant, OTKA 1144, for generous support. We are also grateful to Professor Michael Barfield, Professor Michael Brown, and Dr. Paul Marchetti for their helpful discussions. Computer facilities were provided by the University of Arizona Computer Graphics Facility and Professor Michael F. Brown. We also thank Dr. K. E. Kover for her help in implementing the model free approach, Professor Jozef Kowalewski, and the journal reviewers for their helpful suggestions and valuable comments on the manuscript.

JA934202P

(40) Simon, E. S.; Bednarski, M. D.; Whitesides, G. M. *J. Am. Chem. Soc.* **1988**, *110*, 7159.